



ORIGINAL ARTICLE

Unfolded protein response markers Grp78 and eIF2alpha are upregulated with increasing alpha-synuclein levels in Lewy body disease

Dominik Hrabos^{1,2,3}  | Ilaria Poggiolini¹ | Livia Civitelli¹ | Emilia Galli⁴ |
Chris Espasa⁵ | Mart Saarma⁴ | Päivi Lindholm⁴ | Laura Parkkinen¹ ¹Nuffield Department of Clinical Neuroscience, University of Oxford, Oxford, UK²Department of Clinical and Molecular Pathology, Palacky University Olomouc and University Hospital Olomouc, Olomouc, Czech Republic³Department of Neurology, Palacky University Olomouc and University Hospital Olomouc, Olomouc, Czech Republic⁴Institute of Biotechnology, Helsinki Institute of Life Science, University of Helsinki, Helsinki, Finland⁵Mammalian Genetics Unit, MRC Harwell Institute, Harwell Science and Innovation Campus, Didcot, UK**Correspondence**Laura Parkkinen, Nuffield Department of Clinical Neuroscience, University of Oxford, John Radcliffe Hospital, West wing, Level 6, Oxford OX3 9DU, UK.
Email: laura.parkkinen@ndcn.ox.ac.uk**Funding information**

The study is supported by Ministry of Health, Czech Republic – conceptual development of research organization MH CZ-DRO (FNOL, 00098892); supported by Palacky University Olomouc (IGA_LF_2024_010 and IGA_LF_2024_021). Laura Parkkinen is supported by Parkinson's UK (G-1806), Weston Brain Institute, the Michael J. Fox Foundation (MJFF-019580), Parkinson's Foundation (PF-IMP-941400) and NIHR Oxford Biomedical Research Centre (BRC).

Abstract**Aims:** Endoplasmic reticulum stress followed by the unfolded protein response is one of the cellular mechanisms contributing to the progression of α -synuclein pathology in Parkinson's disease and other Lewy body diseases. We aimed to investigate the activation of endoplasmic reticulum stress and its correlation with α -synuclein pathology in human post-mortem brain tissue.**Methods:** We analysed brain tissue from 45 subjects—14 symptomatic patients with Lewy body disease, 19 subjects with incidental Lewy body disease, and 12 healthy controls. The analysed brain regions included the medulla, pons, midbrain, striatum, amygdala and entorhinal, temporal, frontal and occipital cortex. We analysed activation of endoplasmic reticulum stress via levels of the unfolded protein response-related proteins (Grp78, eIF2 α) and endoplasmic reticulum stress-regulating neurotrophic factors (MANF, CDNF).**Results:** We showed that regional levels of two endoplasmic reticulum-localised neurotrophic factors, MANF and CDNF, did not change in response to accumulating α -synuclein pathology. The concentration of MANF negatively correlated with age in specific regions. eIF2 α was upregulated in the striatum of Lewy body disease patients and correlated with increased α -synuclein levels. We found the upregulation of chaperone Grp78 in the amygdala and nigral dopaminergic neurons of Lewy body disease patients. Grp78 levels in the amygdala strongly correlated with soluble α -synuclein levels.**Conclusions:** Our data suggest a strong but regionally specific change in Grp78 and eIF2 α levels, which positively correlates with soluble α -synuclein levels. Additionally, MANF levels decreased in dopaminergic neurons in the substantia nigra. Our research suggests that endoplasmic reticulum stress activation is not associated with Lewy pathology but rather with soluble α -synuclein concentration and disease progression.**KEYWORDS**

alpha-synuclein, ER stress, Lewy body disease, Parkinson's disease, unfolded protein response

This is an open access article under the terms of the [Creative Commons Attribution](https://creativecommons.org/licenses/by/4.0/) License, which permits use, distribution and reproduction in any medium, provided the original work is properly cited.© 2024 The Author(s). *Neuropathology and Applied Neurobiology* published by John Wiley & Sons Ltd on behalf of British Neuropathological Society.

INTRODUCTION

Parkinson's disease (PD) is a progressive, neurodegenerative disease, pathologically confirmed by loss of dopaminergic neurons in the substantia nigra pars compacta (SNpc) and intracellular aggregation of α -synuclein (aSyn) protein in neuronal cell bodies (Lewy bodies [LBs]), and processes (Lewy neurites [LNs]) in selectively vulnerable brain regions [1]. A major constituent of both structures is aSyn fibrils with interspersed vesicular membranes and organelles [2, 3]. These neuronal structures are pathological hallmarks of LB disease (LBD), which includes PD, Parkinson's disease dementia (PDD), and dementia with Lewy bodies (DLB), that show considerable clinical and pathological overlap. Within LBD, aSyn pathology progressively affects the nervous system in a caudal-to-rostral direction over the course of the disease in six pathologically distinctive stages as described by Braak et al. (Braak stage 1–6) [4]. Even after years of focused research, we still do not fully understand what causes aSyn to aggregate and propagate throughout the brain and how this relates to the underlying neuronal loss [5, 6]. The potential culprits for neurodegeneration include inflammation, oxidative stress, mitochondrial dysfunction, dysregulation of calcium homeostasis and chronic endoplasmic reticulum (ER) stress-induced apoptosis [7]. Accumulation of misfolded proteins such as aSyn results in ER stress and is detected by specific sensors in the ER, collectively known as the unfolded protein response (UPR) [8]. The UPR consists of three pathways, which include ER-resident transmembrane proteins, known as protein kinase RNA-like ER kinase (PERK), inositol-requiring enzyme 1 α (IRE1 α) and activating transcription factor 6 (ATF6) (Figure 1). Upon ER stress, chaperone Grp78 binds to misfolded proteins within the ER, releasing these three signal transducers and allowing their activation [9]. Activation of PERK, IRE1 α and ATF6 promotes the control of the expression of genes encoding factors that modulate ER-associated protein degradation [10], increases biogenesis of the ER and Golgi complex and inhibits protein synthesis, thus preventing an overload of protein in the ER [11]. If the UPR fails to protect a cell from excessive ER stress, it ultimately promotes apoptosis, for example, via upregulation of CHOP [12], ASK1 and NF- κ B [13].

Two ER-localised neurotrophic factors, cerebral dopamine neurotrophic factor (CDNF) and its conserved homologue, mesencephalic astrocyte-derived neurotrophic factor (MANF), have been shown to protect and restore the function of dopaminergic neurons in the rodent and non-human primate models of PD [14–16]. CDNF increases the expression of UPR proteins, such as Grp78, ATF4 and ATF6, and simultaneously decreases terminal UPR pathway protein CHOP during ER stress [17]. Furthermore, CDNF is protective in cultured cells against toxic aSyn oligomers [18] and recently reduced the neuronal internalisation of preformed aSyn fibrils in both in vitro and in vivo models of PD, alleviating also behavioural alterations [19]. Expression of MANF is upregulated after ER stress initiation [20–22]. MANF also functions as a chaperone in the ER [23] and can act as an independent anti-apoptotic agent [24].

Evidence that the UPR is involved in aSyn pathology has primarily been provided by cellular and animal models for PD [25–32].

Key Points

- Regional levels of endoplasmic reticulum-localised neurotrophic factors MANF and CDNF did not change in response to accumulating α -synuclein pathology in the striatum and entorhinal cortex.
- The concentration of MANF negatively correlated with age in cortical regions of Lewy body disease patients.
- Total eIF2 α protein levels and phospho-eIF2 α /total eIF2 α ratio strongly positively correlated with α -synuclein levels in the striata of Lewy body disease patients.
- Grp78 is upregulated in the amygdala and its level is strongly correlated with soluble α -synuclein.
- Upregulation of ER stress markers is associated with levels of soluble α -synuclein rather than Lewy pathology.

Numerous studies have shown that the aggregation of misfolded aSyn induces chronic ER stress and UPR activation in vitro [29, 31] and in vivo [12, 29–31]. The UPR could be proposedly induced by direct interaction between misfolded aSyn and intraluminal ER chaperone Grp78 [29]. Although most of this evidence is experimental, human post-mortem studies have also suggested the role of UPR in the progression of PD. Increased expression of Grp78 has been described in aSyn pathology-affected neurons [33]. Furthermore, the activation of the UPR has also been observed by immunohistochemistry for phosphorylated PERK and eIF2 α in the SNpc neurons of PD patients [34].

In our study, we aimed to further dissect the role of ER stress in LBD-affected brains by systematically analysing the potential activation of the UPR in different stages of the disease. Our initial hypothesis was that we would observe sequential upregulation of UPR markers in subsequently affected regions in both incidental LB disease (ILBD) subjects and LBD patients in response to the progression of Lewy pathology. Thus, we aimed to correlate the results with Braak staging. We focused on MANF and CDNF, as these molecules could have therapeutic potential for neurodegeneration in the future. Furthermore, we hypothesised that there is a direct correlation between Grp78 levels, PERK pathway activation and progressive accumulation of aSyn in the human brain. The regions examined were selected based on their pathological importance in the progression of LBD in the brain.

MATERIAL AND METHODS

Human tissue samples

Post-mortem brain tissue from 45 subjects in total was selected from the Oxford Brain Bank (OBB) for this study. Subjects were selected as symptomatic LBD (PD/PDD/DLB) patients with Braak stages 5–6 aSyn pathology ($n = 14$), subjects with ILBD with Braak stages 1–4

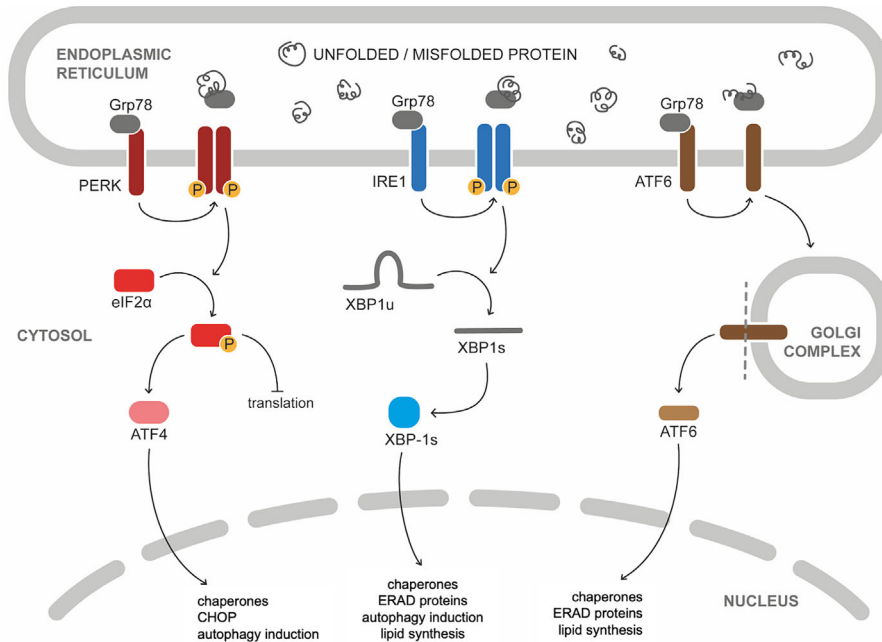


FIGURE 1 Signalling pathways of the unfolded protein response. Accumulation of unfolded or misfolded protein in endoplasmic reticulum (ER) cisternae will eventually resolve in unfolded protein response (UPR), which is controlled by three main ER-resident sensors— protein kinase RNA-like ER kinase (PERK), inositol-requiring enzyme 1 α (IRE1 α) and activating transcription factor 6 (ATF6). After dissociation with Grp78, both PERK and IRE1 α are activated by autophosphorylation. PERK phosphorylates eIF2 α , decreasing protein translation initiation and thus overload of misfolded proteins in ER cisternae. PERK phosphorylation also leads to the translation of ATF4, a transcription factor that promotes the expression of genes related to autophagy and apoptosis (e.g., CHOP). Activation of IRE1 α catalyses the excision of an intron from ubiquitously expressed XBP1u mRNA, causing a frameshift in the XBP1 coding sequence resulting in the translation of XBP-1s, a transcriptional factor that upregulates genes involved in protein folding and quality control, in addition to regulating lipid synthesis. Upon activation, ATF6 is translocated to the Golgi complex, where it is proteolytically cleaved and released as a transcription factor which directs the expression of genes encoding chaperones, ERAD components and molecules involved in lipid synthesis.

aSyn pathology ($n = 19$) and healthy controls ($n = 12$). The patients were selected based on limited concomitant Tau pathology, absence of other neurodegenerative or demyelinating diseases, limited vascular/ischaemic pathology of the brain and absence of malignancy. Brain samples were obtained and prepared in accordance with the Ethics Committee of the University of Oxford (ref 23/SC/0241). Analyses were undertaken on nine different brain regions—medulla, pons, mid-brain, striatum, amygdala and entorhinal, temporal, frontal and occipital cortex. Essential demographic and neuropathological data are shown in Table S1. A summary of the regions used in each experiment is shown in Table S2.

Enzyme-linked immunosorbent assay analysis

For enzyme-linked immunosorbent assay (ELISA), frozen brain tissue samples were homogenised in ice-cold lysis buffer (137-mM NaCl, 20-mM Tris-HCl, 2.5-mM EDTA, 1% NP-40, 10% glycerol, 0.5-mM sodium orthovanadate and cOmplete™ Mini EDTA-free Protease Inhibitor Cocktail [Roche]; pH 8.0) using 0.1 ml of lysis buffer per 10 mg of tissue and plastic pestles. Homogenised samples were incubated for 30 min on ice, centrifuged at 12,000 rpm for 20 min at +4°C and supernatants were collected and stored at -75°C until

analysis. Total protein concentration in the samples was measured using DC Protein Assay (Bio-Rad). The levels of MANF and CDNF were analysed with in-house ELISA [35, 36]. Briefly, MaxiSorp (Nunc) immunosorbent 96-well plates were coated overnight at +4°C with 1 μ g/ml of goat anti-human MANF pAb (R&D Systems, AF3748), or mouse anti-human CDNF mAb (Icosagen, 301-100, clone 7D6), diluted into 50-mM carbonate coating buffer (15mM sodium carbonate, 35-mM sodium bicarbonate, pH 9.6). The plates were then washed with washing buffer (PBS with 0.05% Tween) and blocked with blocking buffer (1% casein [Sigma C8654] in washing buffer for MANF, 3% BSA [Probumin® Merck Millipore] for CDNF, respectively) for 2 h at room temperature. After blocking and subsequent washing, recombinant human (rh)MANF (Icosagen, P-101-100) and rhCDNF (Icosagen, P-100-100) as reference standards, and study samples in blocking buffer were applied in duplicates on wells and incubated overnight at +4°C. Plates were washed four times and incubated with horseradish peroxidase (HRP)-linked mouse anti-MANF mAb (Icosagen, clone 4E12) and HRP-linked mouse anti-CDNF mAb (Icosagen, 302-100, clone 6G5) detection antibodies respectively at 1- μ g/ml concentration for 5 h at room temperature. The plates were finally incubated with 3,3',5,5'-tetramethylbenzidine according to the manufacturer's protocol using DuoSet ELISA Development Systems reagents (R&D Systems, DY999). The absorbances were

quantified by measurement at 450 and 540 nm for background correction using VICTOR3 spectrophotometer (Perkin Elmer). All antibodies and samples were applied to the plate in 100- μ l volume while washing and blocking steps were performed in 200- μ l volume. Brain lysates were analysed as 1:200 for MANF and 1:10 for CDNF. For MANF ELISA the limit of detection (LOD) indicating assay sensitivity was 45 pg/ml, the lower limit of quantitation (LLOQ) 62.5 pg/ml and the dynamic range 62.5–2000 pg/ml. For the in-house CDNF ELISA, the LOD was 31 pg/ml, the LLOQ was 31.3 pg/ml and the dynamic range was 31.3–2000 pg/ml. The mean intra-assay and inter-assay variations analysed as three different concentrations were 8.1% and 5.5% CV for MANF and 7.1% and 8.8% CV for CDNF. MANF ELISA did not cross-react with human recombinant CDNF, or vice versa, even at the highest tested concentration of 500 ng/ml. Recovery of recombinant protein added as 100-pg/ml spike to the study samples was $106.7\% \pm 7.0\%$ (range 99.6%–115.6%, $n = 5$) for MANF ELISA and $98.7\% \pm 10.4\%$ (range 82.6%–110.6%, $n = 5$) for CDNF ELISA. Concentrations were normalised to the total protein concentration in the sample.

Capillary Western blot procedure

For capillary western blot (WB), frozen brain tissue was homogenised in lysis buffer (5mM HEPES, 320mM sucrose, 1mM EDTA, 0.1% SDS; pH 7.4) to 6% w/v. Pierce Protease and Phosphatase Inhibitor Mini Tablets without EDTA (ThermoFisher) were added according to the manufacturer's protocol. The homogenates were spun at $10,000 \times g$ for 10 min at 4°C. The total protein amount in the supernatant was determined using the BCA Protein Quantification Kit (Abcam) and adjusted to 2 mg/ml. Analyses were performed using the Protein Simple Peggy Sue System according to the manufacturer's instructions using a 12–230 kDa separation module (ProteinSimple, SM-S001) and the anti-rabbit (ProteinSimple, DM-001) or the anti-mouse

(ProteinSimple, DM-002) detection modules. Brain homogenates were diluted with sample buffer, then combined with 5 \times fluorescent Master Mix (sample buffer, fluorescent standard, 200-mM DTT) and heated at 95°C for 5 min. The denatured samples, blocking reagent, primary antibodies, the mouse and rabbit HRP-conjugated secondary antibodies, and the chemiluminescent substrate were dispensed into a 384-well plate. After plate loading, the separation electrophoresis and immunodetection steps took place in the fully automated Peggy Sue Western blot system (ProteinSimple), electropherograms were inspected and areas under the curve were statistically analysed. All the results were normalised using β -actin. Additionally, results from the striatum were normalised to tyrosine hydroxylase (TH) levels, as indicated in the results. The antibodies and their dilutions used with Peggy Sue are listed in Table 1.

WB procedure

Protein samples were prepared using 0.5 g of frozen human brain tissue. Tissue was homogenised and fractionated according to sarkosyl-based protocol [37, 38]. Briefly, tissue was homogenised in extraction buffer with sarkosyl (10-mM Tris-HCL, 0.8-M NaCl, 1-mM EGTA, 10% sucrose, 2% sarkosyl; 20 ml/1 g), EDTA-free Pierce Protease and Phosphatase Inhibitor Mini Tablet (ThermoFisher) was added, then incubated at 37°C for 30 min and centrifuged at $10,000 \times g$ in 4°C for 10 min. Supernatants were spun at $21,000 \times g$ at 4°C for 90 min, and the resulting supernatant consisting of soluble fraction 1 (S1 fraction) was collected. The remaining pellets were resuspended in extraction buffer and, after a quick spin, diluted three-fold in sarkosyl buffer (50-mM Tris-HCL, 0.15-M NaCl, 10% sucrose, 0.2% sarkosyl), and they were spun again at $21,000 \times g$ in 4°C for 90 min. The resulting supernatant consisting of soluble fraction 2 (S2 fraction) was collected. Protein concentration was established using Pierce™ BCA Protein Assay Kit (ThermoFisher, 23225). Twenty

TABLE 1 List of antibodies used in Peggy Sue capillary WB, WB, IHC and IF.

Antibody	Host	Manufacturer (Cat. no.)	Dilution	Use
Anti- α -synuclein (Syn1)	Mouse	BD Transduction Lab (#610787)	1:50 1:2000	Peggy Sue WB WB
Anti-tyrosine hydroxylase	Rabbit	Novus Biologicals (NB300-109)	1:50	Peggy Sue WB
Anti-phospho-eIF2 α (Ser51)	Rabbit	Cell Signalling (#3597)	1:50	Peggy Sue WB
Anti-eIF2 α	Rabbit	Cell Signalling (#9722)	1:50	Peggy Sue WB
Anti- β -Actin	Mouse	Abcam (ab8224)	1:100 1:20,000	Peggy Sue WB WB
Anti-Grp78	Rabbit	Abcam (ab21685)	1:2000	WB
Anti-Grp78	Rabbit	Invitrogen (PA1-014A)	1:4000 1:2000	IHC IF
Anti-MANF	Rabbit	Icosagen (310-100)	1:4000	IHC
Anti- α -synuclein (Syn-1, 42)	Mouse	BD Transduction Lab (#610787)	1:1000	IF
Anti- α -synuclein (SynO4)	Mouse	In-house	1:1000	IF

Abbreviations: IF, immunofluorescence; IHC, immunohistochemistry; WB, western blot.

micrograms of each protein sample were loaded onto 7.5% Mini-PROTEAN® TGX™ Precast Gels (Bio-Rad) for protein separation, then transferred to nitrocellulose membrane (Amersham). The membranes were incubated with anti-Grp78 and anti-MANF primary antibodies followed by an HRP-conjugated goat anti-rabbit secondary antibody. Each membrane was probed for β -actin to normalise the levels of immunolabelling. The primary antibodies and their relative dilutions used with WB are listed in Table 1. ECL™ Prime Western Blotting System (Cytiva, RPN2232) was used for developing the membrane. Image analysis and band quantification were performed using ImageJ—we analysed signal intensity as area under the curve.

Immunohistochemistry and immunofluorescence

Immunohistochemistry (IHC) and immunofluorescence (IF) were performed on formalin-fixed and paraffin-embedded midbrain tissue sections (6 μ m) according to a standardised protocol. Briefly, antigen retrieval was performed by either sodium citrate (pH 6) or EDTA buffer (pH 8) using a microwave oven for Grp78 and MANF respectively, and formic acid treatment for aSyn. For aSyn, we have used two antibody clones—Syn-1 (42) and SynO4. The primary antibodies were incubated overnight at 4°C. Dilutions used are given in Table 1. IHC was performed using a REAL EnVision Detection System (Agilent, K500711-2). Quantification of IHC signals was performed using ImageJ following Leica Aperio AT2 whole slide scanning. Ten high-resolution photographs of regions of interest (ROIs) (each with an area of 96,000 μ m²) of one representative subject from each group were taken using Aperio ImageScope software. At least five neurons (diameter over 10 μ m) were present in every region. DAB colour channel was analysed in 8-bit greyscale for mean optical density in the neurons in the ROI. For IF, goat anti-rabbit conjugated with Alexa Fluor 488 (1:200, Invitrogen, A11070) and goat anti-mouse conjugated with Alexa Fluor 568 (1:200, Invitrogen, A11019) secondary antibodies were used. Slides were coverslipped and mounted using an anti-fade mounting medium with DAPI. The signals were visualised using a Zeiss LSM-880 confocal microscope with Airyscan (Carl Zeiss, Germany). Image capture including Z-stack processing was performed using the Zen Black and Zen Blue (Version 3.4, Carl Zeiss, Germany) software. The primary antibodies tested in this study that did not produce a satisfactory result are shown in Table S3.

TaqMan real-time polymerase chain reaction

For real-time polymerase chain reaction (RT-qPCR), total RNA was isolated from 25 mg of tissue using miRNeasy mini kit (Qiagen, 217004) according to the manufacturer's protocol. The yield and quality of the RNA were assessed by measuring the A260:A280 ratio using the NanoDrop One system (ThermoFisher Scientific) according to the standard protocol [39]. Of the purified total RNA, 250 ng was reverse transcribed to cDNA using the SuperScript VILO cDNA Synthesis Kit (ThermoFisher Scientific, 11754050). RT-qPCR analysis was

performed using the Rotor-Gene Q system (Qiagen) and the TaqMan Gene Expression Assays (Applied Biosystems). Reactions were performed in duplicates using the FAM dye-labelled assay. Table S4 lists the used probes. To monitor contamination, each run contained several no-template controls. Each 20- μ l reaction substrate contained 10- μ l TaqMan Universal PCR Master Mix (Applied Biosystems, 4304437), 2- μ l cDNA and 1- μ l TaqMan Probe. The PCR amplification conditions included 2-min initial incubation at 50°C, 10-min denaturation at 95°C followed by heating at 95°C for 15- and 60-s cycles at 40°C. The comparative delta Ct method ($2^{-\Delta\Delta C_t}$ method) was used to calculate the relative fold change in gene expression. Data were normalised to housekeeping genes *GAPDH* and *B2M* to determine ΔC_t and relative expression ($2^{-\Delta C_t}$). Gene expression in the occipital cortex was used as a reference/calibrator for $2^{-\Delta\Delta C_t}$ analysis.

Statistical analysis

Statistical analysis was performed using GraphPad PRISM 8 software. Nonparametric Mann-Whitney *U* test was used for comparison between groups in means or mean-dots columns. Scattered dot plots with linear regression lines were analysed by nonparametric Spearman's rank correlation coefficient calculation. Grubbs' test was performed to identify the outliers. Data points were excluded from the analysis in case of clear analytical errors or discrepancies between duplicates.

RESULTS

ELISA analysis of MANF and CDNF shows no changes during the pathological progression of aSyn pathology, but MANF levels negatively correlate with age

By using in-house ELISAs, we were able to quantify MANF and CDNF levels in human brain tissue. The observed concentrations of MANF (17.6 \pm 4.2, 18.9 \pm 5.5 and 16.8 \pm 3.6 ng/mg total protein in striatum, entorhinal and occipital cortex, respectively) were about 33 times higher than those of CDNF (499.9 \pm 215.9, 554.7 \pm 193.3 and 578.5 \pm 204.3 pg/mg total protein in striatum, entorhinal and occipital cortex, respectively). Protein concentrations of both MANF and CDNF were evenly distributed in LBD, subjects with ILBD and healthy controls in all three examined regions—striatum, entorhinal and occipital cortex. There were no significant changes observed in the concentrations of MANF (Figure 2A) and CDNF (Figure 2B) between groups. Interestingly, we observed a significant negative correlation between MANF concentration and age in the occipital cortex (Figure 2C). Even though there was no significant correlation in the striatum and entorhinal cortex, the trend was similar to the findings in the occipital cortex (Figure 2C). CDNF showed a uniform concentration in the striatum, entorhinal and occipital cortex independently of the age of the subject (Figure 2D). Moreover, we observed that the concentrations of MANF and CDNF were not correlated with each other in any

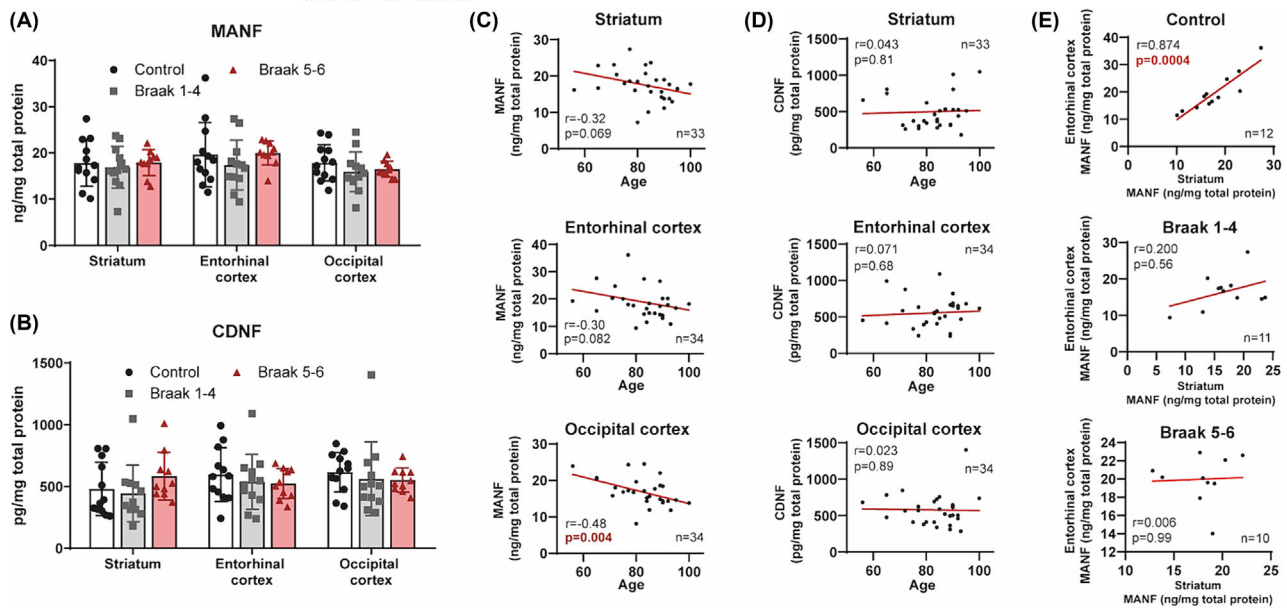


FIGURE 2 The concentration of mesencephalic astrocyte-derived neurotrophic factor (MANF) and cerebral dopamine neurotrophic factor (CDNF) do not change in selected human brain areas. Enzyme-linked immunosorbent assay (ELISA) analysis was used to determine the concentration of MANF (A) and CDNF (B) in tissue homogenates of post-mortem human striatum, entorhinal cortex and occipital cortex in healthy controls ($n = 12$), incidental Lewy body disease (ILBD) subjects (Braak 1–4, $n = 10$ –12) and Lewy body disease (LBD) patients (Braak 5–6, $n = 10$ –11). Correlation between age and protein concentration was analysed for MANF (C) and CDNF (D) in the striatum, entorhinal cortex, and occipital cortex of all subjects. Correlation between MANF concentration in the striatum and entorhinal cortex was analysed in healthy controls (control, $n = 12$), ILBD Braak 1–4 subjects ($n = 11$) and LBD Braak 5–6 patients (Braak, $n = 10$) (E). Means-dots columns \pm SD (A,B) and scattered dot plots (C–E) are shown. Linear regression line (red line), number of pairs (n), Spearman's rank correlation coefficient (r) and p values (p) are shown in the scattered dot plots (C–E). The Mann–Whitney test was used for comparison between groups (A,B). Spearman's rank correlation coefficient was used for correlation analysis (C–E). Significant p values in scattered dot plots are indicated in red.

of the analysed brain regions (data not shown). However, we observed a strong positive correlation between MANF levels in the entorhinal cortex and striatum of healthy controls, which was not present in the analysis of LBD or ILBD (Figure 2E).

Capillary WB shows total eIF2 α to increase in the striatum with the pathological progression of aSyn pathology

Using capillary WB, we analysed eIF2 α and phospho-eIF2 α in the striatum, entorhinal and occipital cortex. We found a significantly higher protein level of total eIF2 α in LBD Braak 5–6 patients than in healthy controls in the striatum (Figure 3A) but not in the entorhinal or occipital cortex. Even though there were no significant differences between ILBD Braak 1–4 subjects and healthy controls in the striatum, there was an observable trend of increased concentration towards the higher Braak stage. Interestingly, we did not observe any significant differences in the concentration of phospho-eIF2 α (Figure 3B) or phospho-eIF2 α to total eIF2 α ratio (Figure 3C) in the striatum between the groups. Importantly, there is a great inter-individual variability, more prominent in the phospho-eIF2 α to total eIF2 α ratios. Further, TH was used in capillary WB to normalise our striatal data, due to its direct correlation with striato-nigral pathway

neurodegeneration. Indeed, we showed that TH levels were significantly lower in LBD Braak 5–6 patients than in healthy controls (Figure 3D). Data analysis of total eIF2 α and phospho-eIF2 α yielded similar results when normalised to TH levels (Figure 3E). Our investigation of the correlation between phospho-eIF2 α and total eIF2 α in the striatum (TH-normalised) showed that levels of these two forms of the protein positively correlate in all three study groups (Figure 3F). This finding was not observed in the entorhinal (Figure 3G) or occipital (data not shown) cortex.

Total eIF2 α protein levels and phospho-eIF2 α /total eIF2 α ratio strongly positively correlate with aSyn levels

Further, we analysed levels of total monomeric aSyn by use of capillary WB in the striatum, entorhinal and occipital cortex. In the striatum, we observed a significantly higher level of aSyn in the ILBD Braak 1–4 group than in healthy controls (Figure 3H). Due to a strong inter-individual variability, LBD Braak 5–6 patients did not consistently show higher levels than controls, but the trend of rising protein levels with the Braak stage is visible (Figure 3H). These trends were similar when we analysed TH-normalised striatal data (Figure 3I). In the entorhinal cortex, we observed that the level of aSyn is

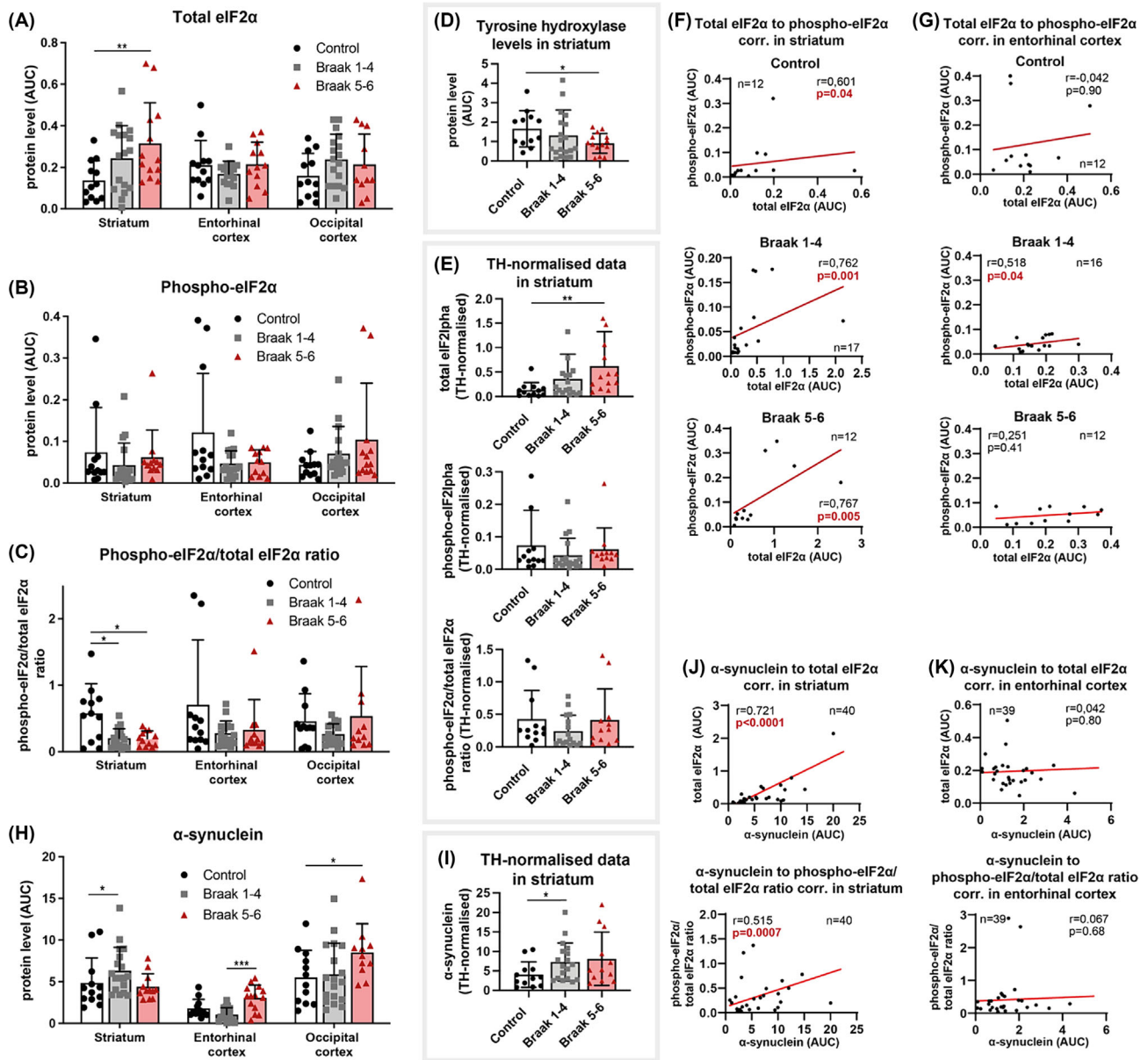


FIGURE 3 Total eIF2 α is upregulated in the striatum of LBD Braak 5–6 patients, phospho-eIF2 α /total eIF2 α ratio positively correlates with aSyn level. Capillary WB analysis was used to determine the relative concentration of total eIF2 α (A), phospho-eIF2 α (B), phospho-eIF2 α /total eIF2 α ratio (C) and aSyn (H) in tissue homogenates of post-mortem human striatum, entorhinal cortex and occipital cortex in healthy controls (control, $n = 12$), ILBD subjects (Braak 1–4, $n = 16$ –18) and LBD patients (Braak 5–6, $n = 11$ –13). Levels of tyrosine hydroxylase (TH) in the striatum were analysed by capillary WB (D) in brain homogenates of healthy controls (control, $n = 12$), ILBD subjects (Braak 1–4, $n = 19$) and LBD patients (Braak 5–6, $n = 14$). Levels of total eIF2 α , phospho-eIF2 α , phospho-eIF2 α /total eIF2 α ratio and aSyn in the striatum were normalised to TH levels (E,I). Total eIF2 α and phospho-eIF2 α level correlation were analysed in the striatum (F) and entorhinal cortex (G) in healthy controls, ILBD Braak 1–4 subjects and LBD Braak 5–6 patients. Correlations between aSyn levels and total eIF2 α levels or phospho-eIF2 α /total eIF2 α ratios were analysed in the striatum (J) and entorhinal cortex (K) of all subjects. Correlation analysis in striatum tissue was performed on TH-normalised data (F,G,J,K). Means \pm SD with individual data points (A–E,H,I) and scattered dot plots (F,G,J,K) are shown. Linear regression line (red line), number of pairs (n), Spearman's rank correlation coefficient (r) and p values (p) are shown in the scattered dot plots. The Mann–Whitney test was used for comparison between groups. Spearman's rank correlation coefficient was used for correlation analysis. Significant p values in scattered dot plots are indicated in red. * $p < 0.05$; ** $p < 0.01$.

significantly higher in LBD Braak 5–6 patients than in ILBD Braak 1–4 subjects. Similarly, significant differences were present in the occipital cortex, between LBD patients and healthy controls (Figure 3H). Finally, our analysis of data from the striatum (TH-normalised) has

shown that there is a strong positive correlation between aSyn levels and both total eIF2 α and phospho-eIF2 α to total eIF2 α ratio (Figure 3J). We did not observe similar results in the entorhinal cortex (Figure 3K).

WB analysis shows that Grp78 is upregulated in LBD patients in the amygdala and its positive correlation with aSyn levels

We used WB to analyse Grp78 protein levels in the S1 fraction of protein homogenates of six regions—medulla, pons, amygdala,

striatum, temporal and frontal cortex. Levels of Grp78 were significantly increased in the amygdala of LBD Braak 5–6 patients compared with the control group (Figure 4A,B). We then correlated the levels of Grp78 with increasing levels of soluble aSyn (Figure 4C), with results showing a strongly significant positive correlation of the proteins in the amygdala (Figure 4D). Medulla (Figure 4E,I), pons (data not shown)

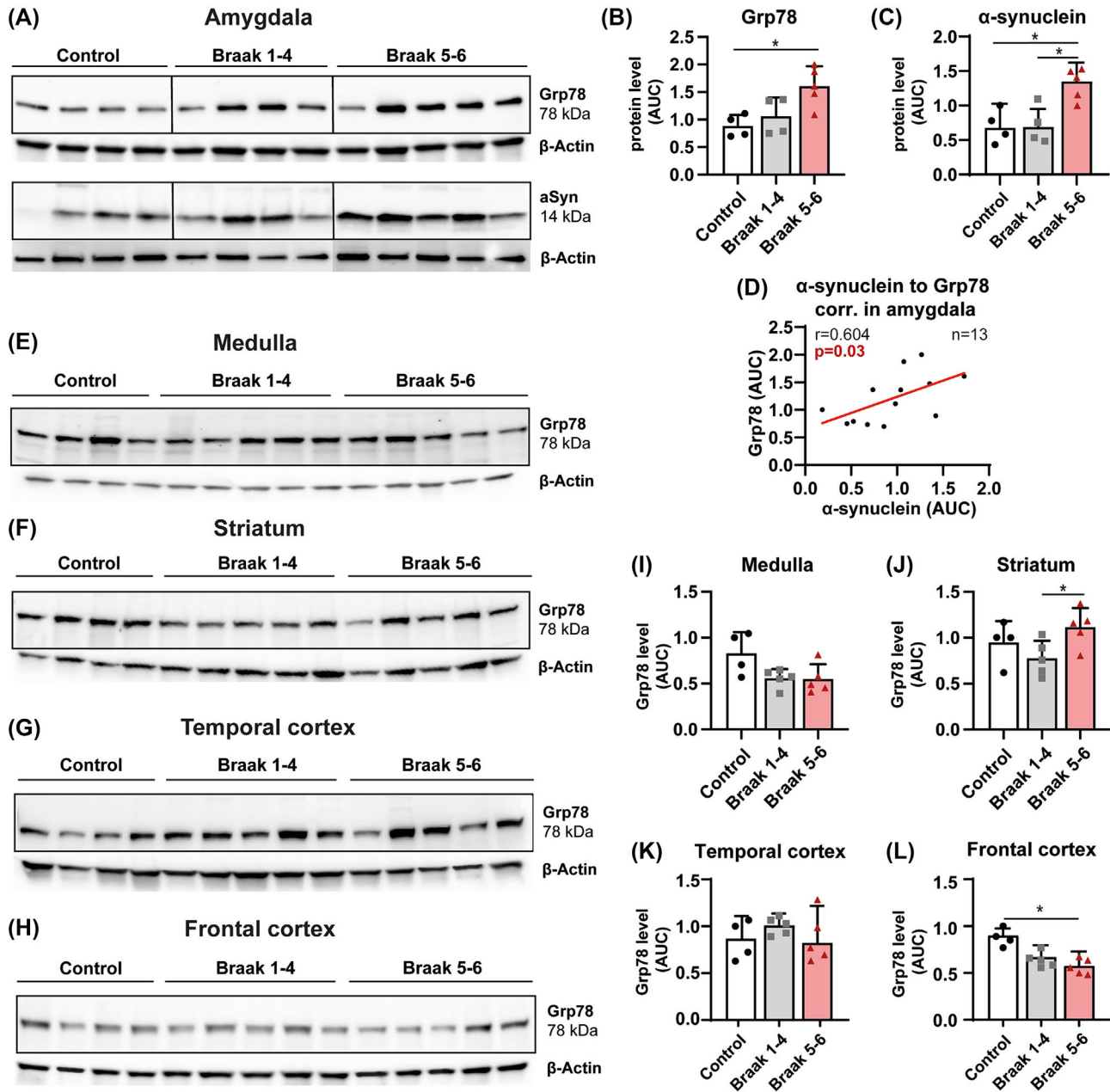


FIGURE 4 Grp78 is upregulated in the amygdala of Lewy body disease (LBD) Braak 5–6 patients and positively correlates with soluble aSyn levels. Relative concentration of Grp78 was determined by Western blot (WB) analysis in amygdala (A,B), medulla (E,I), striatum (F,J), temporal cortex (G,K) and frontal cortex (H,L) in post-mortem brain tissue homogenates of healthy controls ($n = 4$), ILBD Braak 1–4 subjects ($n = 4$ –5) and LBD Braak 5–6 patients ($n = 5$). Grp78 protein level was determined in S1 fraction and normalised to β -actin. The relative concentration of aSyn was determined by WB analysis only in the amygdala (A,C); it was normalised to β -actin. The correlation between Grp78 and aSyn levels was analysed (D). Representative photographs of blots are shown (A,E–H). Means \pm SD with individual data points (B,C,I–L) and a scattered dot plot (D) are shown. Linear regression line (red line), number of pairs (n), Spearman's rank correlation coefficient (r) and p values (p) are shown in the scattered dot plot. The Mann–Whitney test was used for comparison between groups. Spearman's rank correlation coefficient was used for correlation analysis. Significant p -value in the scattered dot plot is indicated in red. * $p < 0.05$.

and temporal cortex (Figure 4G,K) analyses showed no significant changes in Grp78 levels. Further, we observed a significant increase in Grp78 levels in the striatum in LBD Braak 5–6 patients compared with ILBD Braak 1–4 subjects (Figure 4F,J). Frontal cortex data showed a significant decrease in Grp78 levels in LBD patients compared with healthy controls (Figure 4H,L). The comparison of the Grp78 levels clustered according to subject groups shows a pattern of upregulation in the striatum and amygdala with growing Braak stage (Figure 51A). Additionally, we analysed the striatum for soluble aSyn level in S1 fraction with results similar to those obtained by using capillary WB method. There was a significant increase in ILBD Braak 1–4 group compared with healthy controls (Figure 51B). Lastly, comparable results for all regions respectively were observed in an analysis of the S2 fraction in all brain areas (Figure 52A–L).

RT-qPCR analysis showed no significant changes in the gene expression of ER stress markers during the pathological progression of aSyn pathology

We analysed genes that take part in all three crucial UPR pathways. PERK pathway was analysed by quantifying mRNA levels of *EIF2S1* (protein eIF2 α) and *ATF4*. There were no significant changes in mRNA levels in these genes in the striatum (Figure 5A) or entorhinal cortex (Figure 5B) between the controls, ILBD subjects and LBD patients. The same was true for the *ATF6* and *ERN1* (protein IRE1 α), with no significant changes between the groups in both brain regions (Figure 5A,B). Further, we measured levels of mRNA of *DDIT3* (protein

CHOP) and *NFE2L2*, gene coding protein Nrf2, which promotes cell survival following ER stress and UPR pathway activation [40]. Once again, we did not discover any significant changes in mRNA levels of *DDIT3* and *NFE2L2* (Figure 5A,B). Lastly, we analysed the mRNA levels of three UPR-associated neurotrophic factors: *MANF*, *CDNF* and *GDNF* and observed no significant changes in gene expression of these three markers either. Noticeable in-group inter-individual changes in mRNA levels were observed, as demonstrated by high SD, in both striatum and entorhinal cortices (Figure 5A,B).

IHC analysis shows increased levels of GRP78 and decreased levels of MANF in the SNpc dopaminergic neurons with the pathological progression of aSyn pathology

To observe the activation of ER stress in the dopaminergic neuron population of SNpc, we used IHC to analyse Grp78 and MANF immunoreactivity. Grp78 showed increased immunoreactivity in LBs-containing and LBs-free dopaminergic neurons in SNpc of LBD Braak 5–6 patients compared with the expression observed in ILBD subjects (Figure 6A,C). We showed a decreased immunoreactivity for MANF in both ILBD Braak stage 1–4 subjects and LBD Braak stage 5–6 patients compared with controls (Figure 6B). These findings were quantified and showed a significant decrease with the progression of Braak stage (Figure 6D). Interestingly, the results were not restricted to LBs-containing cells but were observed in most of the neuromelanin-containing neurons.

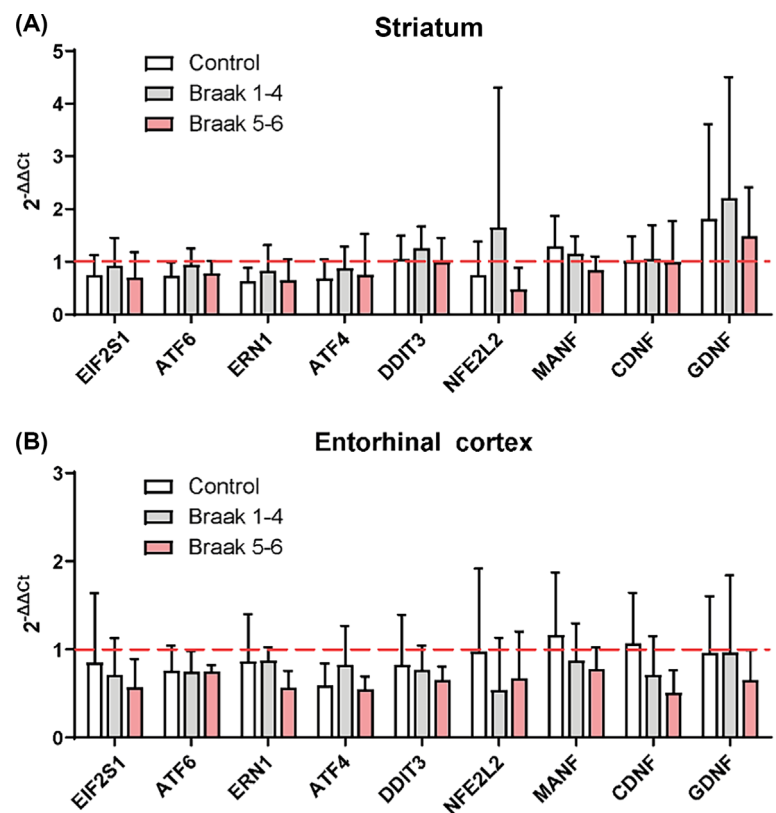


FIGURE 5 Relative mRNA levels of unfolded protein response (UPR)-associated genes. Real-time polymerase chain reaction (RT-qPCR) analysis was used to determine relative fold changes in expression of nine genes (*EIF2S1*, *ATF6*, *ERN1*, *ATF4*, *DDIT3*, *NFE2L2*, *MANF*, *CDNF* and *GDNF*) in post-mortem human brain tissue of healthy controls ($n = 6-8$), incidental Lewy body disease (ILBD) Braak 1–4 subjects ($n = 6$), Lewy body disease (LBD) Braak 5–6 patients ($n = 7-8$). Analysed areas were the striatum (A) and entorhinal cortex (B). Gene expression in the occipital cortex was used as a reference/calibrator for $2^{-\Delta\Delta C_t}$ analysis. Experiments were performed in duplicates. Means \pm SD (A,B) are shown. The Mann–Whitney test was used for comparison between groups.

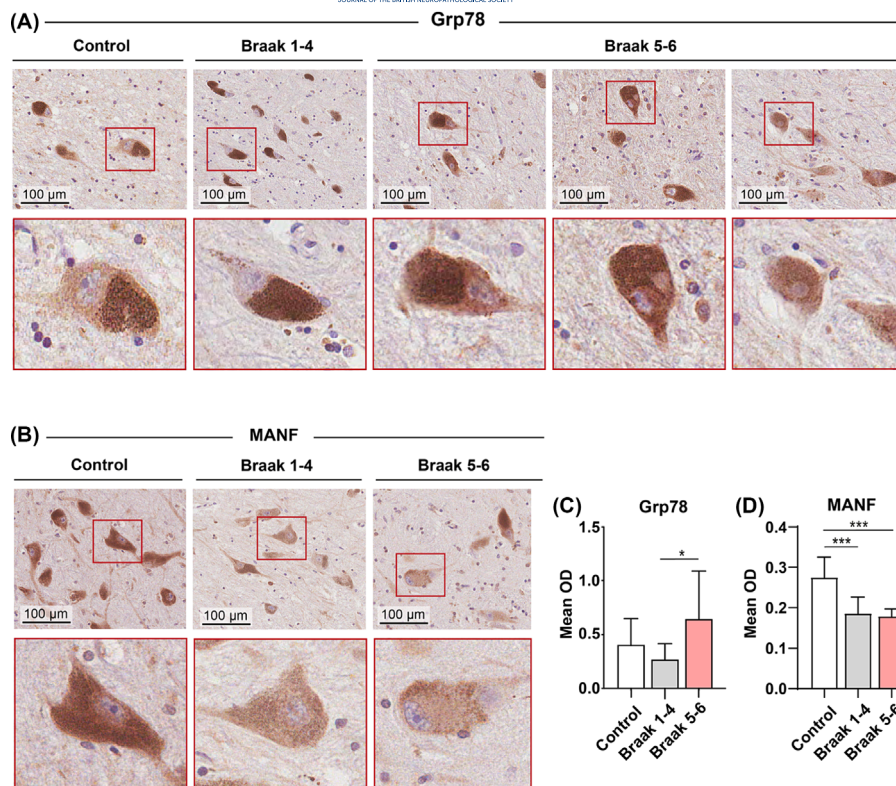


FIGURE 6 Grp78 is upregulated and MANF is downregulated in SNpc dopaminergic neurons in Braak stage 5–6 patients. IHC analysis for Grp78 (A) and MANF (B) was performed in SNpc of healthy controls ($n = 3$), ILBD Braak 1–4 subjects ($n = 2$ –3) and LBD Braak 5–6 patients ($n = 3$) (A). Analysis of the optical density of immunopositive staining (DAB) for MANF (C) and Grp78 (D) was performed in 10 areas within SNpc in a scanned microscope at least twice with similar results. Representative microphotographs (A,B) and means \pm SD (C,D) are shown. The Mann–Whitney test was used for comparison between groups (B,D). * $p < 0.05$; *** $p < 0.001$.

Co-localization of Grp78 and aSyn was observed only rarely in double IF in the SNpc

Intracellular co-localisation of Grp78 with aSyn in SNpc dopaminergic neurons was tested with double IF using two different primary antibodies for the detection of aSyn deposition. With Syn-1 (against epitopes 91–99aa), apart from confirming the findings from IHC, showing that Grp78 is upregulated in SNpc LBD patients compared with controls, we also observed that Grp78 co-localised with aSyn only rarely, and exclusively around the outer layer of the fully developed LBs (Figure 7A). Detailed image in 3D tomogram can be seen in Figure S3. However, using another conformation-specific anti-aSyn antibody (clone SynO4), we found no co-localisation in the SNpc LBs in LBD patients (Figure 7B).

DISCUSSION

There is growing pathological evidence that ER stress plays an important role in LBD pathophysiology. Here, we studied the largest cohort analysed for some of the UPR markers presented so far, including three groups of subjects—symptomatic LBD patients, subjects with ILBD and healthy controls. With this cohort, we could examine the pathological progression of aSyn pathology, given the different Braak stages used. We hypothesised that there would be a correlation between ER-localised neurotrophic factors and ER stress markers with progressive accumulation of aSyn in the LBD human brain, and we

employed several techniques to investigate this. There has been a lack of high-quality testing of several primary antibodies in human brain tissue. Therefore, our first effort was to analyse commercially available primary antibodies for use in human-centred neuropathological research. We used very sensitive, in-house-built ELISA for neurotrophic factors, MANF and CDFN, which were not detectable using conventional WB and commercially available antibodies (data not shown). Capillary WB allowed us to analyse tissue samples in a more high-throughput manner; however, the availability of optimised primary antibodies was a limitation. Conventional WB proved to be an ideal method for the detection of abundant proteins, such as Grp78. Moreover, we employed IHC to specifically examine MANF and Grp78 expression in the dopaminergic SNpc neurons in situ. Although we carefully selected ROIs to avoid analytical errors, the presence of neuromelanin could influence optical density levels. Lastly, we decided to analyse mRNA expression by RT-qPCR. Degradation of mRNA due to prolonged post-mortem delay is a major issue that must be taken into consideration when interpreting the presented data as it could explain noticeable inter-individual changes in mRNA levels within the study groups.

Despite the earlier findings in vitro and in vivo on the possible relationship between CDFN and MANF with ER stress and aSyn aggregation [18, 19], our study observed no significant differences in the levels of either neurotrophic factor during the progressive accumulation of aSyn pathology. We also failed to draw any correlations between CDFN and MANF ELISA levels and total soluble aSyn or markers of ER stress (eIF2 α , Grp78) measured with capillary or

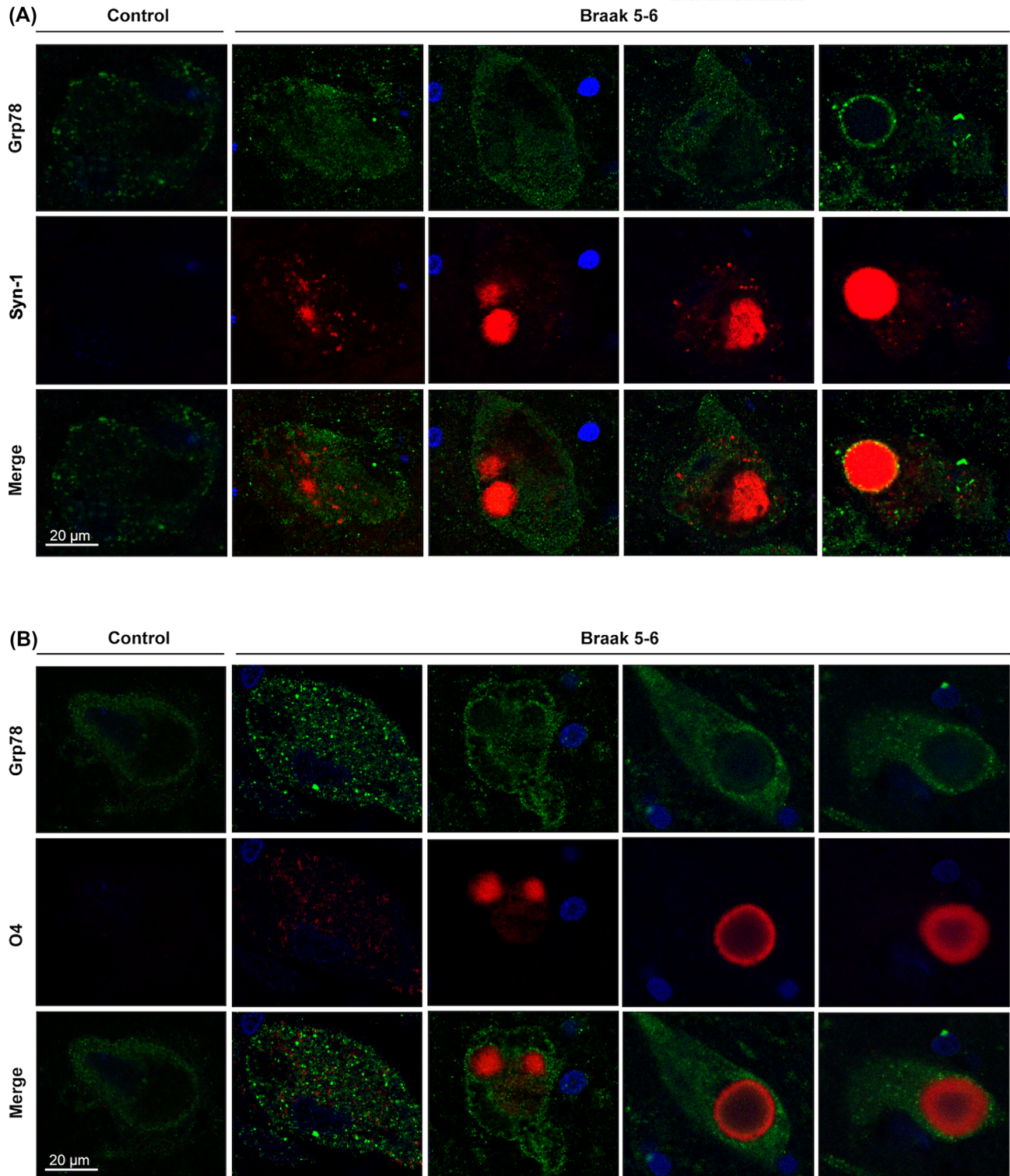


FIGURE 7 Co-localization analysis of Grp78 and aSyn in SNpc in human brain. Double immunofluorescence (IF) analysis of Grp78 (green) and aSyn (red) was performed in SNpc of healthy controls (control, $n = 2$) and Braak 5–6 subjects (Braak 5–6, $n = 4$) (A,B). Two clones of aSyn antibodies were used in two consecutive experiments—Syn-1 (A) and SynO4 (B). Cell nuclei are stained with DAPI (blue). The z-stacking method was used to analyse the pictures using confocal microscopy. Each picture represents an individual 0.35- μ m section.

conventional WB. This may be partly attributed to the sensitivity limitations of the techniques used to investigate these complex interactions. Furthermore, Albert et al. recently suggested a more

complex and nuanced relationship, noting that although the CDF treatment reduced the preformed fibril uptake in their aggregation model of PD, it did not reduce the number of phosphorylated aSyn

inclusions in the SNpc [19]. However, CDNF did inhibit the growth phase of aSyn aggregation *in vitro*, considered to present the misfolded oligomeric aSyn species, and thus, it may have an effect on oligomeric aSyn without affecting the actual inclusion formation. This would warrant further studies examining the relationship between CDNF/MANF and oligomeric species of aSyn either using seed amplification assay or *in situ* technique such as proximity ligation assay. Interestingly, we also showed that MANF levels appeared to decrease with age in the cortex whereas no such correlation was observed for CDNF. The decrease of MANF levels with age has been shown before in human serum [41]. The levels of MANF and CDNF did not correlate with each other overall, but levels of MANF correlated in the entorhinal cortex and striatum in healthy controls and ILBD cases. This relationship was lost in LBD patients with abundant aSyn pathology suggesting an imbalance further along in the progression of the disease process. Importantly, to our knowledge, our study is the first to show a decrease in MANF expression in human SNpc neurons with disease progression using IHC analysis, albeit this being done on a small patient group size and further confirmation is necessary.

Out of all the three UPR pathways, the PERK pathway has been mostly investigated in post-mortem PD brains [27, 34, 42]. We found that WB levels of total eIF2 α (but not phosphorylated eIF2 α) were significantly higher in the striatum of LBD patients compared with healthy controls, but not in the entorhinal and occipital cortex. To examine the activation of the PERK pathway, we analysed the phospho-eIF2 α /total eIF2 α ratio, as phosphorylation of eIF2 α indicated protein activation. However, this ratio was not significantly changed in any of the regions analysed. Furthermore, we found the levels of total and phospho-eIF2 α to correlate positively in the striatum of all cases, suggesting that there is probably no dysregulation or disproportionate activation of phosphorylation in response to accumulating aSyn pathology. Our findings align with Baek et al., who reported a significant increase in the level of total eIF2 α in the frontal and temporal cortices of PD patients, while the phospho-eIF2 α levels remained unchanged [42]. In contrast, Mercado et al. reported a clear increase in the levels of both phosphorylated PERK and eIF2 α in both PD and ILBD cases in several brain areas [27]. Hoozemans et al. and Mercano et al. have also analysed the PERK pathway more specifically in the SNpc neurons using IHC and showed phospho-PERK and phospho-eIF2 α positivity in LBD patients, but not in control cases. However, only up to 20% of the aSyn-positive neurons in SNpc of PD patients showed increased phospho-PERK immunoreactivity, and it appeared to have a different subcellular localization from aSyn [34]. We did not observe any differences in the mRNA level of eIF2 α in any examined regions, consistent with Baek et al., who also found stable mRNA despite the changes in the eIF2 α protein levels [42].

The key role in the activation and modulation of the UPR response lies with intraluminal ER chaperones, including Grp78. To study the relative concentration of Grp78 by WB, we analysed brain homogenates in all major affected brain regions in PD. We observed very different patterns of Grp78 expression in response to disease progression in different brain areas. We found significantly lower

levels of Grp78 protein in the frontal cortex of LBD subjects compared with controls whereas no differences were observed in the pons, medulla and temporal cortex. In contrast, in the amygdala, we observed a significant increase in Grp78 levels in LBD patients compared with controls. Baek et al. found decreased levels in the frontal cortex but also in the cingulate gyrus and temporal cortex. Moreover, we found the Grp78 levels to positively correlate to the level of total aSyn in the amygdala.

Two main approaches to tissue homogenisation were used during the WB analysis—whole cell homogenates in capillary WB and soluble fractions in conventional WB. Interestingly, aSyn levels in the striatum analysed by both techniques were quite similar. Thus, our results are transferable independently of the used tissue processing technique. In the analysis, we have used antibody clones with epitopes only rarely affected by truncation or phosphorylation, which thus showed us a comprehensive picture of the total soluble aSyn level, independent of the posttranslational changes of the aSyn.

Accumulation of unfolded and specifically misfolded aSyn protein affects protein trafficking at multiple stages. Misfolded proteins are prone to form toxic oligomeric aSyn forms, which can bind to biological membranes, including ER cisternae. [43, 44]. To further examine the relationship of UPR proteins and distinct aSyn aggregates, we examined expression levels *in situ* in the dopaminergic SNpc cells during the progression of the disease and the co-localization of Grp78 with aSyn aggregates. Consistent with findings by Credle et al., we found an increased Grp78 expression in the pigmented neurons of the SNpc with the progressing aSyn pathology. However, we showed that the Grp78 expression was mostly punctate throughout the cell and did not associate with the developing aSyn aggregates. Co-localisation of Grp78 was only seen rarely and almost exclusively around the outer layer of the fully developed LBs, suggesting that UPR activation and aSyn aggregates formation are not associated.

The precise chain of events leading to UPR activation remains unclear and has not yet been described in detail. Many studies have suggested that LBs and LNs are not necessarily linked to neurodegeneration, by showing no correlation between LBs formation and neuronal loss [6, 45]. In short, neurodegeneration occurs independently of LB formation. Our data further support this hypothesis showing that UPR upregulation can also be LBs independent. We only observed UPR upregulation (increased Grp78 and eIF2 α) in SNpc, striatum and amygdala and not in the other regions also affected by LBs (medulla, pons, temporal and frontal cortex). We believe that the UPR response is not automatically increased in response to LB formation *per se* but can be found in certain vulnerable areas where the upregulation correlates with soluble aSyn. Furthermore, our finding of *in situ* upregulation of Grp78 in SNpc neurons without LBs suggests the same hypothesis. Therefore, we believe that soluble forms of aSyn, rather than LBs could be an answer to ER stress activation.

A deeper understanding of UPR mechanisms in the human brain is crucial for developing new therapeutic approaches. There is a series of molecules targeting UPR pathways, some of which are proving to be effective in slowing the progression of neurodegeneration in

models, including GSK2606414 [46] and ISRIB [47]. Additionally, the repurposed drugs trazodone hydrochloride and dibenzoylmethane have proved to have a neuroprotective effect both in tauopathy-frontotemporal dementia mice by inhibiting UPR activation [48]. A phase I/II randomised, placebo-controlled, double-blinded, multi-centre clinical study in patients with advanced PD with intraputamenal CDNF injection was completed in August 2020, with results showing CDNF to achieve its primary endpoint of safety and tolerability [49]. Thus, research on the interplay between UPR and aSyn pathology holds the potential to fill an acute need for targeted therapy in neurodegenerative diseases.

ETHICS STATEMENT

All participants gave informed consent for their tissue to be used in research and the study had ethics approval from the UK National Research Ethics Service. The use of tissue material in Finland was approved by a regional Ethics Committee of the Hospital District of Helsinki and Uusimaa.

AUTHOR CONTRIBUTIONS

Dominik Hrabos performed the analyses and drafted the manuscript. Dominik Hrabos, Ilaria Poggolini, Livia Civitelli, Mart Saarna, Emilia Galli and Chris Esapa performed experiments. Laura Parkkinen, Päivi Lindholm and Mart Saarna participated in the conceptualization, experimental design and study coordination. All authors read the manuscript, provided comments on the draft and approved the final version.

ACKNOWLEDGEMENTS

We thank all the donors and their families for their invaluable brain donation to the Oxford Brain Bank. The Oxford Brain Bank is supported by the Medical Research Council (MRC), Brains for Dementia Research (BDR) (Alzheimer Society and Alzheimer Research UK), Autistica UK and the National Institute for Health Research (NIHR) Oxford Biomedical Research Centre. Further, we thank the laboratory staff of the contributing centres and institutes. Additionally, we thank Alan King Lun Liu for his essential help with confocal microscopy analysis, which was performed at the Dunn School Bioimaging Facility at the University of Oxford.

CONFLICT OF INTEREST STATEMENT

Päivi Lindholm and Mart Saarna are inventors in the CDNF-related and MANF-related patents (7,452,969; 9,592,270) owned by Herantis Pharma Plc. M. S. is a minority shareholder in Herantis Pharma Plc. Other authors declare that they have no competing interests.

DATA AVAILABILITY STATEMENT

The data that support the findings of this study are available from the corresponding author upon reasonable request.

ORCID

Dominik Hrabos  <https://orcid.org/0000-0001-9856-0126>

Laura Parkkinen  <https://orcid.org/0000-0002-3392-8564>

REFERENCES

- Dickson DW, Braak H, Duda JE, et al. Neuropathological assessment of Parkinson's disease: refining the diagnostic criteria. *Lancet Neurol.* 2009;8(12):1150-1157. doi:10.1016/S1474-4422(09)70238-8 Retraction in: *Lancet Neurol.* 2010 Jan;9(1):29
- Shahmoradian SH, Lewis AJ, Genoud C, et al. Lewy pathology in Parkinson's disease consists of crowded organelles and lipid membranes. *Nat Neurosci.* 2019;22(7):1099-1109. doi:10.1038/s41593-019-0423-2
- Wakabayashi K, Tanji K, Odagiri S, Miki Y, Mori F, Takahashi H. The Lewy body in Parkinson's disease and related neurodegenerative disorders. *Mol Neurobiol.* 2013;47(2):495-508. doi:10.1007/s12035-012-8280-y
- Braak H, Del Tredici K, Rüb U, de Vos RA, Jansen Steur EN, Braak E. Staging of brain pathology related to sporadic Parkinson's disease. *Neurobiol Aging.* 2003;24(2):197-211. doi:10.1016/s0197-4580(02)00065-9
- Parkkinen L, Pirttilä T, Alafuzoff I. Applicability of current staging/categorization of alpha-synuclein pathology and their clinical relevance. *Acta Neuropathol.* 2008;115(4):399-407. doi:10.1007/s00401-008-0346-6
- Parkkinen L, O'Sullivan SS, Collins C, et al. Disentangling the relationship between lewy bodies and nigral neuronal loss in Parkinson's disease. *J Parkinsons Dis.* 2011;1(3):277-286. doi:10.3233/JPD-2011-11046
- Mercado G, Valdés P, Hetz C. An ERcentric view of Parkinson's disease. *Trends Mol Med.* 2013;19(3):165-175. doi:10.1016/j.molmed.2012.12.005
- Walter P, Ron D. The unfolded protein response: from stress pathway to homeostatic regulation. *Science.* 2011;334(6059):1081-1086. doi:10.1126/science.1209038
- Hetz C. The unfolded protein response: controlling cell fate decisions under ER stress and beyond. *Nat Rev Mol Cell Biol.* 2012;13(2):89-102. Published 2012 Jan 18. doi:10.1038/nrm3270
- Acosta-Alvear D, Zhou Y, Blais A, et al. XBP1 controls diverse cell type- and condition-specific transcriptional regulatory networks. *Mol Cell.* 2007;27(1):53-66. doi:10.1016/j.molcel.2007.06.011
- Hetz C, Saxena S. ER stress and the unfolded protein response in neurodegeneration. *Nat Rev Neurol.* 2017;13(8):477-491. doi:10.1038/nrneuro.2017.99
- Urria H, Dufey E, Lisbona F, Rojas-Rivera D, Hetz C. When ER stress reaches a dead end. *Biochim Biophys Acta.* 2013;1833(12):3507-3517. doi:10.1016/j.bbamcr.2013.07.024
- Hu P, Han Z, Couvillon AD, Kaufman RJ, Exton JH. Autocrine tumor necrosis factor alpha links endoplasmic reticulum stress to the membrane death receptor pathway through IRE1alpha-mediated NF-kappaB activation and down-regulation of TRAF2 expression. *Mol Cell Biol.* 2006;26(8):3071-3084. doi:10.1128/MCB.26.8.3071-3084.2006
- Lindholm P, Saarna M. Novel CDNF/MANF family of neurotrophic factors. *Dev Neurobiol.* 2010;70(5):360-371. doi:10.1002/dneu.20760
- Lindholm P, Voutilainen MH, Laurén J, et al. Novel neurotrophic factor CDNF protects and rescues midbrain dopamine neurons in vivo. *Nature.* 2007;448(7149):73-77. doi:10.1038/nature05957
- Voutilainen MH, Bäck S, Peränen J, et al. Chronic infusion of CDNF prevents 6-OHDA-induced deficits in a rat model of Parkinson's disease. *Exp Neurol.* 2011;228(1):99-108. doi:10.1016/j.expneurol.2010.12.013
- Arancibia D, Zamorano P, Andrés ME. CDNF induces the adaptive unfolded protein response and attenuates endoplasmic reticulum stress-induced cell death. *Biochim Biophys Acta Mol Cell Res.* 2018;1865(11 Pt A):1579-1589. doi:10.1016/j.bbamcr.2018.08.012
- Latge C, Cabral KM, de Oliveira GA, et al. The solution structure and dynamics of full-length human cerebral dopamine neurotrophic factor and its neuroprotective role against alpha-Synuclein oligomers. *J Biol Chem.* 2015;290(33):20527-20540. doi:10.1074/jbc.M115.662254

19. Albert K, Raymundo DP, Panhelainen A, et al. Cerebral dopamine neurotrophic factor reduces α -synuclein aggregation and propagation and alleviates behavioral alterations in vivo. *Mol Ther*. 2021; 29(9):2821-2840. doi:10.1016/j.ymthe.2021.04.035
20. Mizobuchi N, Hoseki J, Kubota H, et al. ARMET is a soluble ER protein induced by the unfolded protein response via ERSE-II element. *Cell Struct Funct*. 2007;32(1):41-50. doi:10.1247/csf.07001
21. Tadimalla A, Belmont PJ, Thuerauf DJ, et al. Mesencephalic astrocyte-derived neurotrophic factor is an ischemia-inducible secreted endoplasmic reticulum stress response protein in the heart. *Circ Res*. 2008; 103(11):1249-1258. doi:10.1161/CIRCRESAHA.108.180679
22. Lindholm P, Peränen J, Andressoo JO, et al. MANF is widely expressed in mammalian tissues and differentially regulated after ischemic and epileptic insults in rodent brain. *Mol Cell Neurosci*. 2008; 39(3):356-371. doi:10.1016/j.mcn.2008.07.016
23. Henderson MJ, Richie CT, Airavaara M, Wang Y, Harvey BK. Mesencephalic astrocyte-derived neurotrophic factor (MANF) secretion and cell surface binding are modulated by KDEL receptors. *J Biol Chem*. 2013;288(6):4209-4225. doi:10.1074/jbc.M112.400648
24. Eesmaa A, Yu LY, Göös H, et al. The cytoprotective protein MANF promotes neuronal survival independently from its role as a GRP78 cofactor. *J Biol Chem*. 2021;296:100295. doi:10.1016/j.jbc.2021.100295
25. Ryu EJ, Harding HP, Angelastro JM, Vitolo OV, Ron D, Greene LA. Endoplasmic reticulum stress and the unfolded protein response in cellular models of Parkinson's disease. *J Neurosci*. 2002;22(24): 10690-10698. doi:10.1523/JNEUROSCI.22-24-10690.2002
26. Smith WW, Jiang H, Pei Z, et al. Endoplasmic reticulum stress and mitochondrial cell death pathways mediate A53T mutant alpha-synuclein-induced toxicity. *Hum Mol Genet*. 2005;14(24):3801-3811. doi:10.1093/hmg/ddi396
27. Mercado G, Castillo V, Soto P, Sidhu A. ER stress and Parkinson's disease: pathological inputs that converge into the secretory pathway. *Brain Res*. 2016;1648(Pt B):626-632. doi:10.1016/j.brainres.2016.04.042
28. Heman-Ackah SM, Manzano R, Hoozemans JJM, et al. Alpha-synuclein induces the unfolded protein response in Parkinson's disease SNCA triplication iPSC-derived neurons. *Hum Mol Genet*. 2017; 26(22):4441-4450. doi:10.1093/hmg/ddx331
29. Bellucci A, Navarria L, Zaltieri M, et al. Induction of the unfolded protein response by α -synuclein in experimental models of Parkinson's disease. *J Neurochem*. 2011;116(4):588-605. doi:10.1111/j.1471-4159.2010.07143.x
30. Colla E, Coune P, Liu Y, et al. Endoplasmic reticulum stress is important for the manifestations of α -synucleinopathy in vivo. *J Neurosci*. 2012;32(10):3306-3320. doi:10.1523/JNEUROSCI.5367-11.2012
31. Cooper AA, Gitler AD, Cashikar A, et al. Alpha-synuclein blocks ER-Golgi traffic and Rab1 rescues neuron loss in Parkinson's models. *Science*. 2006;313(5785):324-328. doi:10.1126/science.1129462
32. Sugeno N, Takeda A, Hasegawa T, et al. Serine 129 phosphorylation of alpha-synuclein induces unfolded protein response-mediated cell death. *J Biol Chem*. 2008;283(34):23179-23188. doi:10.1074/jbc.M802223200
33. Credle JJ, Forcelli PA, Delannoy M, et al. α -Synuclein-mediated inhibition of ATF6 processing into COPII vesicles disrupts UPR signaling in Parkinson's disease. *Neurobiol Dis*. 2015;76:112-125. doi:10.1016/j.nbd.2015.02.005
34. Hoozemans JJ, van Haastert ES, Eikelenboom P, de Vos RA, Rozemuller JM, Scheper W. Activation of the unfolded protein response in Parkinson's disease. *Biochem Biophys Res Commun*. 2007; 354(3):707-711. doi:10.1016/j.bbrc.2007.01.043
35. Galli E, Härkönen T, Sainio MT, et al. Increased circulating concentrations of mesencephalic astrocyte-derived neurotrophic factor in children with type 1 diabetes. *Sci Rep*. 2016;6(1):29058. Published 2016 Jun 30. doi:10.1038/srep29058
36. Galli E, Lindholm P, Kontturi LS, Saarna M, Urtti A, Yliperttula M. Characterization of CDNF-secreting ARPE-19 cell clones for encapsulated cell therapy. *Cell Transplant*. 2019;28(4):413-424. doi:10.1177/0963689719827943
37. Diner I, Nguyen T, Seyfried NT. Enrichment of detergent-insoluble protein aggregates from human postmortem brain. *J vis Exp*. 2017; (128):55835. Published 2017 Oct 24. doi:10.3791/55835
38. Schweighauser M, Shi Y, Tarutani A, et al. Structures of α -synuclein filaments from multiple system atrophy. *Nature*. 2020;585(7825): 464-469. doi:10.1038/s41586-020-2317-6
39. Desjardins P, Conklin D. NanoDrop microvolume quantitation of nucleic acids. *J vis Exp*. 2010;(45):2565. Published 2010 Nov 22. doi: 10.3791/2565
40. Sarcinelli C, Dragic H, Pieczyk M, et al. ATF4-dependent NRF2 transcriptional regulation promotes antioxidant protection during endoplasmic reticulum stress. *Cancers (Basel)*. 2020;12. Published 2020 Mar 1(3):569. doi:10.3390/cancers12030569
41. Sousa-Victor P, Neves J, Cedron-Craft W, et al. MANF regulates metabolic and immune homeostasis in ageing and protects against liver damage. *Nat Metab*. 2019;1(2):276-290. doi:10.1038/s42255-018-0023-6
42. Baek JH, Mamula D, Tingstam B, Pereira M, He Y, Svenningsson P. GRP78 level is altered in the brain, but not in plasma or cerebrospinal fluid in Parkinson's disease patients. *Front Neurosci*. 2019;13:697. Published 2019 Jul 5. doi:10.3389/fnins.2019.00697
43. Nemani VM, Lu W, Berge V, et al. Increased expression of alpha-synuclein reduces neurotransmitter release by inhibiting synaptic vesicle recluster after endocytosis. *Neuron*. 2010;65(1):66-79. doi: 10.1016/j.neuron.2009.12.023
44. Colla E. Linking the endoplasmic reticulum to Parkinson's disease and alpha-synucleinopathy. *Front Neurosci*. 2019;13:560. Published 2019 May 29. doi:10.3389/fnins.2019.00560
45. Iacono D, Geraci-Erck M, Rabin ML, et al. Parkinson disease and incidental Lewy body disease: just a question of time? *Neurology*. 2015; 85(19):1670-1679. doi:10.1212/WNL.0000000000002102
46. Mercado G, Castillo V, Soto P, et al. Targeting PERK signaling with the small molecule GSK2606414 prevents neurodegeneration in a model of Parkinson's disease. *Neurobiol Dis*. 2018;112:136-148. doi: 10.1016/j.nbd.2018.01.004
47. Halliday M, Radford H, Sekine Y, et al. Partial restoration of protein synthesis rates by the small molecule ISRIB prevents neurodegeneration without pancreatic toxicity. *Cell Death Dis*. 2015;6(3):e1672. Published 2015 Mar 5. doi:10.1038/cddis.2015.49
48. Halliday M, Radford H, Zents KAM, et al. Repurposed drugs targeting eIF2 α -P-mediated translational repression prevent neurodegeneration in mice. *Brain*. 2017;140(6):1768-1783. doi:10.1093/brain/awx074
49. Herantis Pharma. CDNF phase I 12-month topline results: safety, UPDRS and DAT PET data. 2020. https://herantis.com/wp-content/uploads/2020/09/200915-CDNF-Webinar_FINAL.pdf. Accessed Nov 3, 2020.

SUPPORTING INFORMATION

Additional supporting information can be found online in the Supporting Information section at the end of this article.

How to cite this article: Hrabos D, Poggolini I, Civitelli L, et al. Unfolded protein response markers Grp78 and eIF2 α are upregulated with increasing alpha-synuclein levels in Lewy body disease. *Neuropathol Appl Neurobiol*. 2024;50(4):e12999. doi:10.1111/nan.12999